

EXPERIMENTAL ANALYSIS OF THE EFFECTS OF SINGLE-PHASE IMMERSION
COOLING OF OPTICAL INTERCONNECTS ON MECHANICAL PROPERTIES OF
ACTIVE OPTICAL CABLES

by

HRISHABH SINGH

Presented to the Faculty of the Graduate School of
The University of Texas at Arlington in Partial Fulfillment
of the Requirements
for the Degree of

MASTER OF SCIENCE IN MECHANICAL ENGINEERING

THE UNIVERSITY OF TEXAS AT ARLINGTON

MAY 2018

Copyright © by Hrishabh Singh 2018

All Rights Reserved



Acknowledgements

I would like to take this opportunity to express my profound gratitude to Dr. Dereje Agonafer for affording me the opportunity to pursue my research goals under his tutelage, and the valuable insight into the power of collaboration between industry and academia.

I would like to thank the IAB & ES2 mentors for their crucial feedback and support for this research project.

I would like to specially thank Dr. Veerendra Mulay from Facebook for his interest and counsel on our project.

I would like to thank Dr. Abdolhossein Haji Sheikh for being part of my thesis defense committee, and even more so for teaching me important concepts of advanced heat transfer during my Master's.

I would like to thank Mr. Jimil Shah for his unrelenting support, patience and guidance throughout the course of this research. I am also grateful to Mr. Ashwin Siddarth for his technical advice and encouragement.

I would also like to thank Ms. Gruebbel and Ms. Wendy Ryan at the MAE Department for their help and support.

Lastly, I would like to thank my parents for inculcating in me the values and attitude to constantly strive to be a better citizen of the world.

May 8, 2018

Abstract

EXPERIMENTAL ANALYSIS OF THE EFFECTS OF SINGLE-PHASE IMMERSION
COOLING OF OPTICAL INTERCONNECTS ON MECHANICAL PROPERTIES OF
ACTIVE OPTICAL CABLES

Hrishabh Singh, MS

The University of Texas at Arlington, 2018

Supervising Professor: Dereje Agonafer

Active optical cables (AOC) are being increasingly adopted for data communication and storage, networking, and high-performance computing (HPC) applications. However, their ability to meet higher data-rate requirements necessitates increased heat dissipation demands in fiberoptic datacom systems. Many dielectric coolants having heat capacities much higher than that of air are available in the market. However, there is a lack of literature and data on the reliability of using single-phase dielectric fluids for immersion-cooling of inter and intra-rack optical interconnections in data centers. Industry standards and prevalent aging test methods for optical cables prove insufficient as they do not address immersion in these coolants.

In this work, the mechanical behavior of an active optical cable (AOC) aged in a single-phase dielectric coolant has been studied. Accelerated aging conditions were achieved by immersing the cable in zero-stress condition in jars containing mineral oil and commercial synthetic engineered fluid placed in a climatic chamber at an elevated temperature for a total duration of 288 hours. Samples were removed every 72 hours for subsequent mechanical testing and microscopy. Scanning Electron Microscopy was used

to assess surface morphology, and the thermomechanical properties were characterized using a Dynamic Mechanical Analyzer (DMA). Necessary comparisons were made with the as-received cable samples. The potential for application of Arrhenius extrapolation method to model temperature-dependent properties of the samples was explored, and mathematical modeling of evolution of the Young's modulus with time was done to understand the degradation attributable to possible chemical interactions between the cable jacket and the engineered fluid.

Table of Contents

Acknowledgements	iii
Abstract	iv
List of Illustrations	viii
List of Tables	x
Chapter 1 INTRODUCTION.....	11
1.1 Application in Data Centers	12
1.1.2 Active Optical Cable (AOC).....	12
1.2 Oil-immersion cooling	15
1.3 MICE and IP Rating for Use in Harsh Environments.....	16
1.4 Reliability Considerations	17
1.4.1 Mechanical Reliability	17
1.4.2 Optical Reliability	19
Chapter 2 THERMAL AGING TEST	21
2.1 Existing Standards.....	21
2.2 Literature Review	21
2.3 ASTM D3455	22
2.4 Aging Temperature and Temperature Profile	22
2.5 Testing Procedure	24
2.6 Temperature Cycling Profile	26
2.7 Physical Observations	26
Chapter 3 DYNAMIC MECHANICAL ANALYSIS	29
3.1. Overview	29

3.2. Apparatus	30
3.3. Specimen Preparation	31
3.4 Observations.....	34
3.5 Results	35
3.5.1. Elastic Modulus (E^*)	35
3.5.2 Loss Tangent.....	41
3.7 Theoretical Treatment of Mechanical Effects of Aging.....	42
3.7.1 Mechanism of Degradation	43
Chapter 4 SURFACE MORPHOLOGY	45
4.1 Scanning Electron Microscope	45
4.2 Cross-section of as-received cable samples	46
4.3 Air-Exposed Sample after 2nd cycle	49
4.4 Mineral Oil-Immersed Sample after 3rd cycle	50
Chapter 5 CONCLUSION AND FUTURE WORK.....	52
References.....	54
Biographical Information	58

List of Illustrations

Figure 1-1 The AOC transceiver and schematic of the host-board connector block pin .. 13

Figure 1-2 FINISAR 10Gbps SFP+ Active Optical Cable 14

Figure 1-3 Communication Channel 17

Figure 1-4 Optical fiber construction 18

Figure 0-5 Refractive index profile..... 18

Figure 0-6 Installation loss along communication channel.....19

Figure 2-1 Test setup in environmental chamber.....24

Figure 2-2 Temperature cycling plot.....25

Figure 2-3 EC-100 before testing.....27

Figure 2-4 EC-100 after 6 weeks..... 27

Figure 2-5 mineral oil before testing..... 28

Figure 2-6 mineral oil after 6 weeks..... 28

Figure 3-1 The DMA used..... 30

Figure 3-2 Air-exposed sample 341

Figure 3-3 Oil-immersed sample.....32

Figure 3-4 Sample-holding jaw and probe.....33

Figure 3-5 Oil-immersed sample after removal from DMA.....34

Figure 3-6 Air-exposed sample after removal from DMA.....34

Figure 3-7 Response of mineral oil-immersed sample scanned at 1 & 5Hz after 2nd cycle
..... 355

Figure 3-8 Response of EC-100-immersed sample @ 1Hz frequency after 4th cycle.....36

Figure 3-9 E-T correlation for fiberoptic temperature sensor..... 37

Figure 3-10 E vs T behavior of mineral oil immersed sample after 3rd cycle.....37

Figure 3-11 E vs T behavior of EC-100 immersed sample after 4th cycle.....	38
Figure 3-12 Evolution of complex/elastic modulus over aging time at DMA furnace temperature of 40°C.....	39
Figure 3-13 Evolution of complex/elastic modulus over aging time at DMA furnace temperature of 22°C.....	40
Figure 3-14 $\tan\delta$ peak shifts with aging time.....	41
Figure 3-15 Elastic modulus vs time for EC-100 immersed samples at 40°C furnace temperature.....	42
Figure 3-16 Elastic modulus vs time for EC-100 immersed samples at 22°C furnace temperature.....	42
Figure 4-1 SEM setup	454
Figure 4-2 View of overall cross section	465
Figure 4-3 Magnified view of core and PVC jacket.....	465
Figure 4-4 One of the two silica cores	476
Figure 4-5 1.2K times magnified view of air-exposed sample	498
Figure 4-6 1.5K times magnified view of air-exposed sample	498
Figure 4-7 2K times magnified view of oil-immersed sample	509
Figure 4-8 1K times magnified view of oil-immersed sample	50
Figure 4-9 1.5K times magnified view of oil-immersed sample	50

List of Tables

Table 1-1 Properties of Mineral and Synthetic Oil Used.....	15
Table 3-1 Specimen elastic modulus vs time at 40°C DMA furnace temperature.....	39
Table 3-2 Specimen elastic modulus vs time at 22°C DMA furnace temperature.....	40
Table 3-3 Loss tangent peaks.....	41

Chapter 1

INTRODUCTION

This report presents an investigation of the potential for using oil-immersion as a technique to cool IT equipment connected via fiberoptic cabling. Oil-immersion as a disruptive, novel technique needs to be better understood, and the aim of this work is to thoroughly survey the potential long-term effects it could have on said equipment.

There is a lack of literature on the challenges posed by the direct influence of oil immersion on various types of IT equipment and this report attempts to respond to these challenges.

Furthermore, with the growing number of applications like cloud computing and search engines hosted by servers requiring intensive interaction between the servers in the data center [1], the communication requirements between racks in the data centers will keep increasing significantly. Network designers have to contend with higher cooling requirements due to increased heat generation and power consumption. There is urgent need to address the increased heat-dissipation required to sustain the growing network traffic in data centers.

Aside from inter-board or inter-rack linking and telecommunications switching systems, optical fibers find increasing application in the following fields:

1. Data cabling for factory automation and plant control equipment
2. Domestic consumer computer-to-peripheral data links, PC bus extension
3. Proprietary LANs
4. Digital video applications
5. Medical instruments
6. Thermometry sensors
7. Automotive networks

Fiberoptic cables offer the benefits of higher bitrates, reduced system weight and susceptibility to electromagnetic interference, which makes them ideal candidates for connecting the growing amount of digital equipment in multimedia applications in automobiles, and other harsh environments.

1.1 Application in Data Centers

A move to high density data center infrastructure places considerable demand on network capability and reliability to meet the demands placed by 10G and higher data-rate infrastructure, easily exceeding the capability of copper-based electrical interconnects. Multimode Fiber (MMF) is the cable-type of choice for meeting the low-latency and high-bandwidth requirements for fiber optic modules to connect servers, switches, and storage devices.

1.1.2 Active Optical Cable (AOC)

Active optical cables (AOCs), a relatively new choice for data transmission networks, are enjoying growing use in data center and telecom central office network cabling. Active Optical Cables are a variant of standard multimode fiber that are preferable for short reach interconnections (intra and inter-rack). One can ascribe their increasing popularity to them offering the high bitrate, reduced weight, and high EMI-resistance that comes with optical fibers and still being simpler to install than pre-terminated or field-terminated cables, which make up the bulk of data center cable infrastructure.

Conventional passive optical cables must have their ends terminated with SC, LC or MPO connectors. These optical connectors, in turn, plug into optical ports on the source and sink device, which is how the electrical-optical signal conversion occurs. AOCs reduce the need for dedicated training to install because of the plug-and-play characteristic of their

electrical design, as visible in the AOC port in figure 1-1. The silver encasings shown in figure 1-1 are referred to as the end modules of the AOC. They constitute the transceiver unit which comprises a semiconductor laser and laser driver for generation of optical signal, and a high-speed photodetector and amplifier for receiving it.

As seen from the orientation in figure 1-1, the optical fibers connect to from the left of the host-board PCB, and couple to the laser or photodetector. This block then connects to the ICs containing laser driver or amplifier, which subsequently connects to the external electrical connector (gold pins).

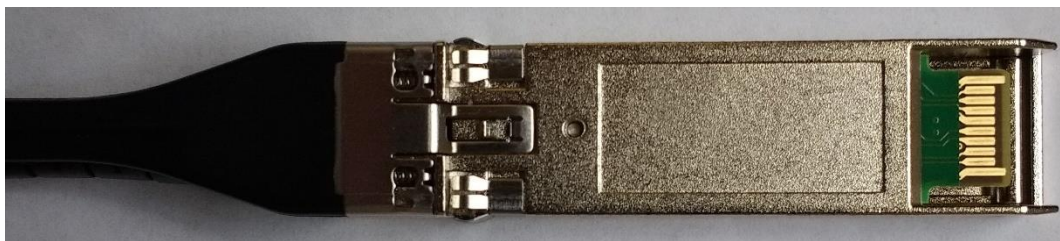
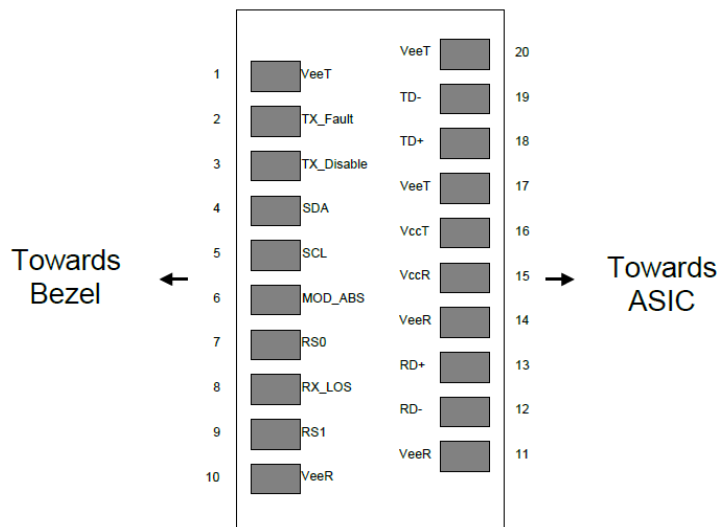


Figure 1-1 The AOC transceiver and schematic of the host-board connector block pin

The AOC tested in this work was a standard glass-core multimode fiber cable procured from Finisar Corporation. Product specifications are as follows:

Silica-based two-circular-core Active Optical Cable

OM2 category multimode fiber (MMF)

10 G ethernet intra and inter-rack applications

0 to 70°C operating range (commercial)

~2.9 mm OD

Total length of 3m

OFNR rated PVC jacket

100 N long term cable tensile load

30 mm long term bend radius



Figure 1-2 FINISAR 10Gbps SFP+ Active Optical Cable

1.2 Oil-immersion cooling

Mineral oil has been extensively used to cool transformers for a long time. Cooling by immersing the device in oil offers multiple benefits, the major ones being simplicity of design and superior thermal properties. As demonstrated in Table 1-1, the heat capacitance, thermal conductivity, and specific heat of mineral and synthetic oil far surpass that of air: this implies substantial reduction in energy consumption, when compared with traditional air-cooled data centers [9,10]. Circumventing the need for airflow paths can allow for increased power densities. Also, the coolant distribution unit for oil is less complicated than that required for water, owing to the variable nature of the chemical composition of the water depending on the source, and the need to better leak-proof due to the inferior dielectric properties compared to oil [11]. All these benefits lend themselves to oil-immersion finding new applications in DIY/hobby/amateur mining operations that generate significant heat.

Table 1-1 Properties of mineral and synthetic oil used

Property	Mineral Oil	EC-100
Density(kg/cu.m) @16°C	870	830
Kinematic Viscosity(cSt) @40°C	9.39	9.58
Specific Heat(J/kgK)	1670	2200
Thermal Conductivity(W/mK)@40°C	0.132	0.1373
CTE (1/K)	0.00064	0.00068
Refractive Index*	1.462	1.453

*RI of pure silica glass is 1.55, RI of cladding of the fiber used is slightly lower. This has implications for the signal attenuation characteristics of the fiber as discussed in section

1.4.2. The mineral oil was supplied by STE Oil Company, and the synthetic fluid, EC-100, was furnished by Engineered Fluids, Texas.

1.3 MICE and IP Rating for Use in Harsh Environments

When reviewing the possibility of damage induced by immersion in oil, the next logical step was to review existing industry standards for rating manufactured cables based on chemical and temperature resistance. The M.I.C.E system classifies fiberoptic cables based on their response to Mechanical, Ingress, Climatic Chemicals, and Electromagnetic stress [12].

Ingress Protection (IP) Code rates equipment on the suitability for continuous immersion in water in conditions that are specified by the manufacturer, and hence although cables rated IP 7 and higher do provide some confidence, there is no justification for following the IP code as a basis for testing in oil-based environments. Test results on the effects of ingress of water, and added conditions such as temperature cycling before immersion that are elucidated in white papers by individual manufacturers are vastly different from the operating conditions that would be encountered by fiberoptic cables immersed in dielectric coolant.

A thorough review of the M.I.C.E analysis system and IP Code can only go so far as to help speculate which cable type(s) would be suited better to the oil environment. However, sole resistance to severe environmental conditions of some of these cables does not guarantee the ability to withstand attack due to continued immersion in oil.

1.4 Reliability Considerations

There are several components of the fiberoptic module in what is known as the communication channel (figure 1-3). The mechanical and optical considerations of their reliability is briefly discussed in the following sections.

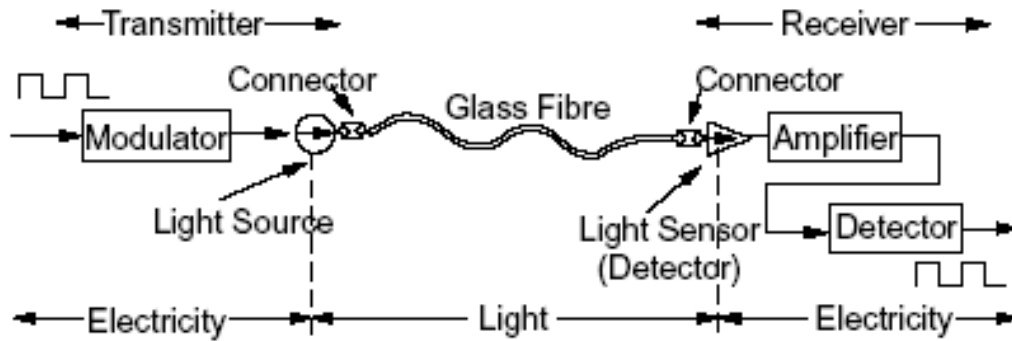


Figure 1-3 Communication Channel

1.4.1 Mechanical Reliability

The reliability of a network would be restricted by the component with the highest likelihood of failure. PCBs, electrical connectors, and some other components have been tested in these dielectric environments [2,3,4,5,6,7,8], but there is no technical literature on the effect of oil-immersion on optical components like transmitter and receiver modules, connectors, cables, splices, etc. that comprise a fiber optic module.

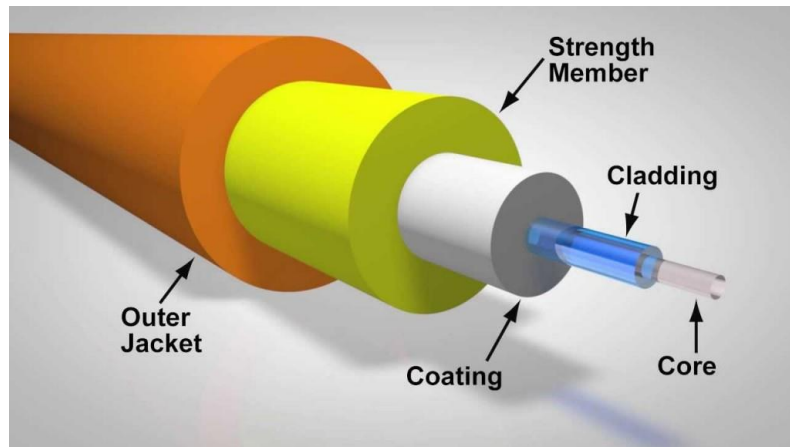


Figure 1-4 Optical fiber construction

The role of cable jackets (figure 1-4) is to protect the glass core from environmental conditions that may affect performance and long-term durability. Coatings around the fiber cladding are a means to ensure the reliability of the transmitted signal and helping minimize attenuation due to microbending. Hence, retention of the ability of each of these layers is not just a mechanical reliability consideration but is also connected to optical reliability as discussed in the next section.

1.4.2 Optical Reliability

In a fiberoptic cable, the electrical signal, upon conversion into an optical signal travels along the core of the fiber surrounded by an optical cladding with a lower refractive index that traps light in the core through total internal reflection. The signal transmission characteristics of an optical fiber are a result of its refractive index profile. As can be inferred from figure 1-4, this profile is a gradient from a higher refractive index (core) to a lower refractive index (cladding). Ingress of oil into this interface would not only change the refractive index profile but also alter the thermophysical properties of the glass, specifically its viscoelastic properties, which are strong functions of temperature. Residual stresses and strains can arise in optical fibers when the optical fiber exhibits thermophysical properties that change over time. Any ingress of oil leading to viscoelastic changes may be followed by a change in the refractive index profile at core-cladding interface. This could cause greatly reduce signal integrity, by affecting the ability of the waveguide's total internal reflection properties.

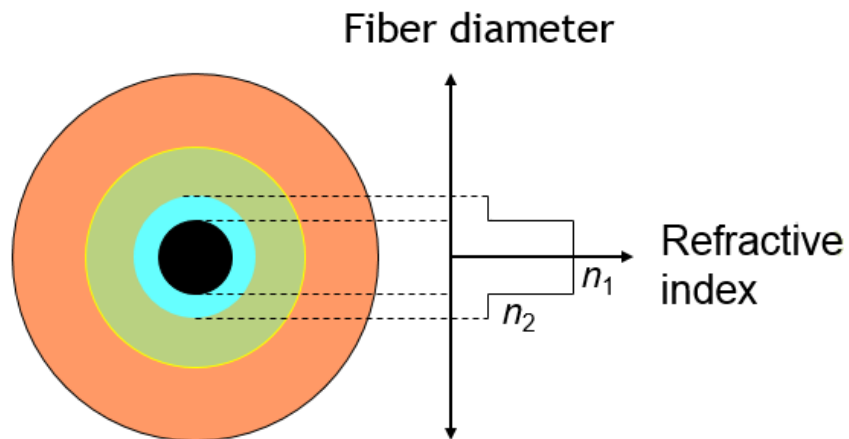


Figure 1-5 Refractive index profile

Potential for losses is especially high at interconnections in the optical fiber communication systems. During regular service conditions, these losses are termed installation losses.

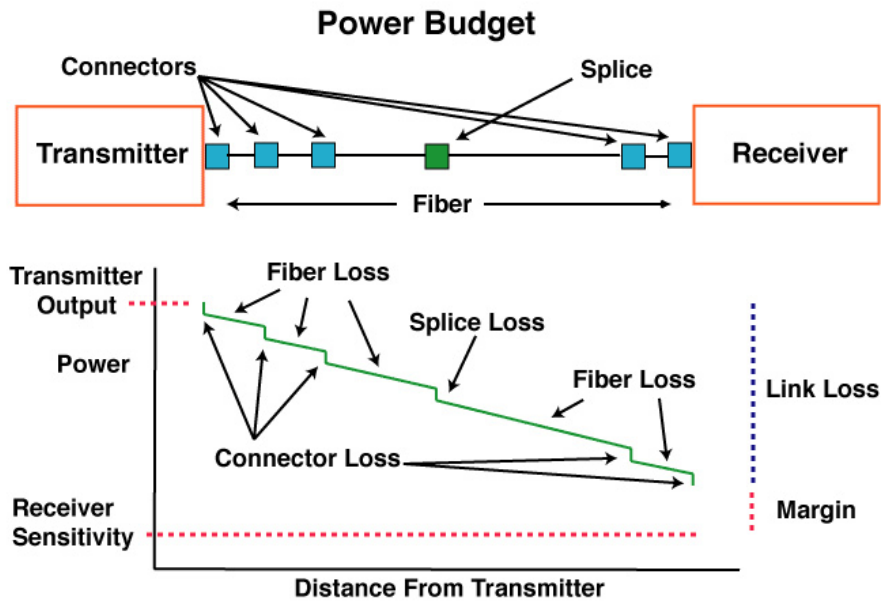


Figure 1-6 Installation loss along communication channel

There is a need to explore if and how these losses increase as a result of oil ingress. Multiple sites along the communication channel, seen in figure may be vulnerable to oil ingress. Cable ends rendered prone to penetration by the coolant serve as the assumption and necessity for our reliability analysis of critical interconnections in oil-immersed optical fiber systems.

In summary, higher equipment density causes higher operating temperatures, and calls for either improved cooling techniques or better temperature-resistant designs and/or materials like polycarbonate cores or Teflon claddings. The aim of this work is to determine whether cooling by immersing in dielectric coolants can meet the increased cooling demands without retrofitting existing designs or compromising reliability.

Chapter 2

THERMAL AGING TEST

Thermal degradation attributable to the chemical and physical processes that occur in polymeric materials at higher temperatures can best be used to evaluate reliability based on a common test method called thermal aging. Elevated temperatures hasten the aging process that may be the result of oxidation, mechanical creep, chemical attack, etc.

2.1 Existing Standards

There are a host of standards in industry, such as JEDEC, ASTM and IEC. However, none of them have laid out any procedures for testing fiberoptic interconnections in mineral or synthetic oil. They mostly exist to establish standardized testing of equipment in air, and not oil. Since, the ramp rates of oil and air are very different, employing these standards would not be wise. IEC 60793 establishes uniform requirements for testing and measuring damp heat 85°C/85% RH, dry heat 85°C, temperature cycling between -60°C and +85°C, and water immersion at 23°C. ASTM D3455 also provides partial but necessary information about testing compatibility of various materials with mineral oil.

An experiment modeled on the basis of a combination of the procedures outlined in all said standards was devised, and the reason for this is laid out in the next section.

2.2 Literature Review

Environmental tests done by Corning on their ClearCurve multimode optical fiber reveal induced attenuation of 0.1 dB/km between -60 and 85°C [24]. However, attenuation induced by water immersion is twice that (0.2) at 23°C, while heat aging at 85°C also causes an attenuation of 0.2 dB/km. Clearly, a tradeoff exists between increased device density caused by immersion cooling and transmission degradation.

The overall mechanical behavior of glass-core fibers is strongly dependent on flaws on the fiber surface [18]. There is an overabundance of literature on high temperature aging and humidity aging tests of silica fiber [19,20] which follow IEC and ASTM standards, and establish that even after severe aging, there is insignificant degradation in fiber strength.

The most comprehensive work on fiber reliability is found in the final report issued in 1999 by COST 246, a European research program that included IEC members. However, none of the results of the tests that constituted that report completely explain or account for the tensile strength increases of 5% after hot-air aging, 15% after hot-filling compound aging, and the increase in the dynamic fatigue parameter (from c. 17 to 30) for these fibers when aged under zero stress at high temperature in cable filling compounds. These were results observed by aging tests of optical fibers done by T. Volotinen et al [21].

This led to this report's preliminary hypotheses that the jacket would harden, coating toughen, and the overall cable stiffen.

2.3 ASTM D3455

The ASTM D3455 standard delineates the methodology to be followed when testing the compatibility of construction material with electrical insulating oil of petroleum origin, otherwise known as mineral oil. The standard was closely followed in carrying out the experiment, with necessary modifications made to account for the lack of information on compatibility testing of fiberoptic cable.

2.4 Aging Temperature and Temperature Profile

Accelerated aging by immersion in oil at an elevated temperature was made to induce new aging processes not experienced by the cable under regular air-cooled data center service

conditions. Hence, the choice of aging temperature and cycling profile of temperature with respect to time was key. Comprehensive accelerated aging tests were done by Dwivedi et al [20] and included immersion in water at aging temperature of 100°C, but by their own admission these were unrealistic aging environments that would never be faced by fibers in service. Temperature cycling tests in air have also been limited to aging the cable jacket and observing the effect on fiber core. However, effect of the aging conditions on the cladding coatings (acrylate) have either been non-existent in most literature or under-reported by the ones that have studied the same [21].

The lifetime model developed for glass-core optical fibers by Griffioen has a temperature dependent strength degradation term $G(ta)$ [22]. The higher the value of $G(ta)$, the greater the effect of the stressor on the fiber lifetime. Griffioen reports that immersion in water at 20 °C gives a value of $G(ta)$ that causes the ratio of applied stress to proof stress to decrease by a factor of 2.15. For fibers that are immersed in water as well as being under strain due to bending, the water causes an effective strain that is 2.15 times greater than the mechanical strain due to the bend radius, e.g. when a fiber is stored at a bend radius of 35 mm it experiences a strain of 0.18%. When stored at 35 mm and immersed in water, the effective strain increases to 0.38%. Thus, it seems that the effect of diffusion of water into the cable structure is the dominant factor in mechanical degradation. This is attested by Glaesemann et al [18].

Williams-Landel-Ferry theory would call for either higher acceleration factor or aging temperature, but to limit ourselves to realistic operation temperatures, and taking into account the limited time, an aging temperature of 45°C was chosen. This closely resembled the choice of aging conditions used by T. Volotinen et al [21]. Temperature cycling profile and duration of testing have been elucidated in the sections that follow. Longer durations of immersion would be ideal as aging time is the most crucial parameter in studying

reliability. Nevertheless, short time aging at high temperature is useful for estimating relative lifetimes of different cables [25].

Relative Humidity setpoint was chosen based on a couple of factors. Since the jars with the oil-immersed cable were covered, RH was irrelevant. Testing all specimens simultaneously ensured that they experienced identical environmental conditions leading to fair and conclusive results. However, for air-exposed samples, 10-15% RH would be ideal. But, as can be inferred from [20], 35% RH corresponding to a 30°C dew point in 45°C dry bulb chamber temperature is low enough to remove moisture as a variable. More importantly, 35% RH is much closer to realistic operating conditions in air-cooled data centers than 10/15% RH.

2.5 Testing Procedure

Three, approximately 50 cm-long sections were cut out from the 3m as-received cable. Studying the effect of immersion on aging of fiber coating necessitated keeping the ends of said sections open and immersed to enable entry of oil. This was tied in with the fact that the environmental stressor (oil in this case) has not been in physical contact with the cladding coating hitherto, as discussed in section 2.4. 3 1L Borosilicate glass jars were used - one filled with mineral oil, another with EC-100 synthetic fluid and one jar is exposed to air, to serve as a control for the effect of immersion. The jars with the dielectric fluids were filled up to the 800 ml mark.

All samples were baked for 4 hours prior to immersion. Each 50 cm section was placed in each of the 3 jars. The dielectric fluid-containing jars are covered and closed tightly. ASTM D3455 standard has been closely followed in carrying out experiment.



Figure 2-1 Test setup in environmental chamber

2.6 Temperature Cycling Profile

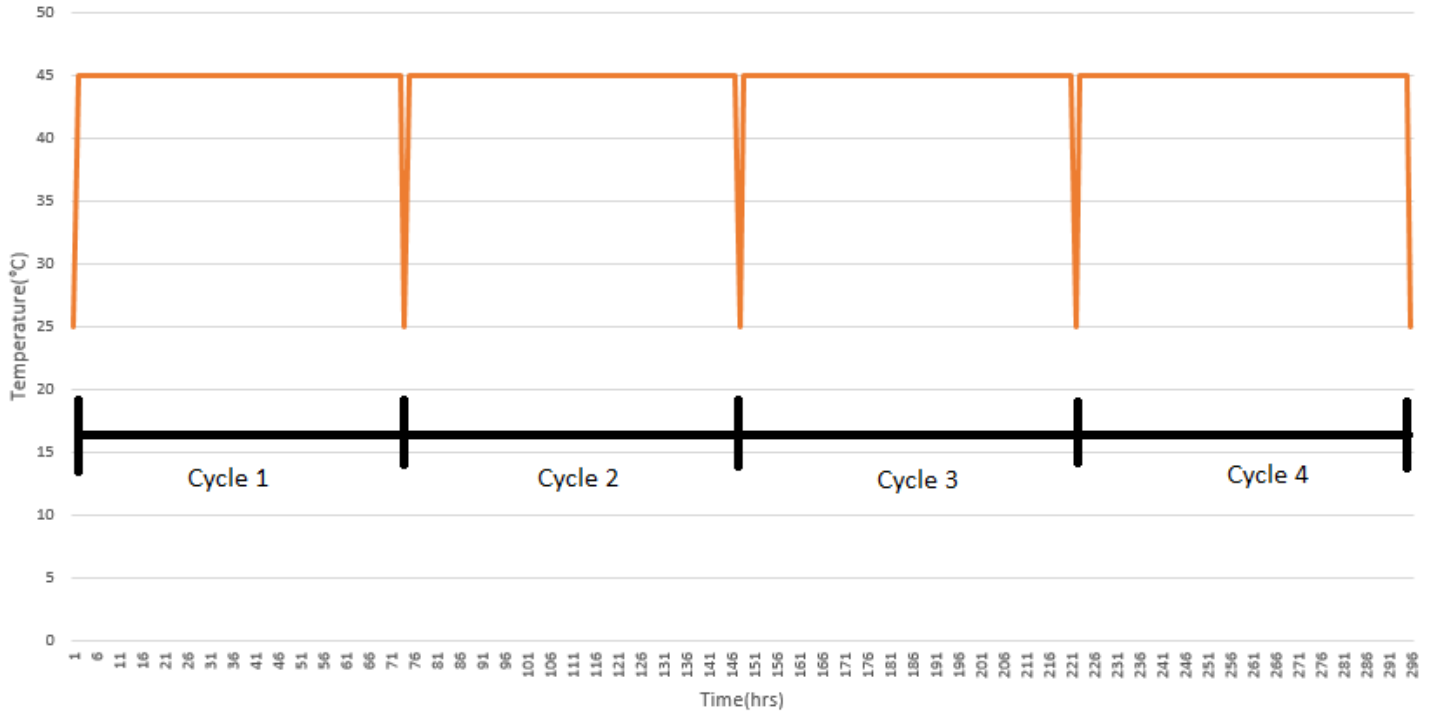


Figure 2-2 Temperature cycling plot

Due to the significant differences in heat capacity between single-phase oil and air resulting in vastly different ramp times, performing an accelerated thermal cycling for oil like it is done for air would be highly impracticable [2]. Therefore, a temperature cycling program more akin to aging at elevated temperatures was chosen and is visualized in the climatic chamber temperature versus aging time plot shown in figure 2-. Thus, the two-faceted goal of simulating long-term effects of realistic service conditions was achieved by accelerated aging at a reasonable temperature for a feasible duration.

2.7 Physical Observations

Both mineral oil and EC-100 were clear and colorless before and during the test. An insignificant amount of oil had evaporated and deposited on jar lids. No noticeable change in color or texture for up to 3 weeks after last test was observed. A slight yellowish tinge was observed in EC-100 5-6 weeks after the last test (4th cycle).

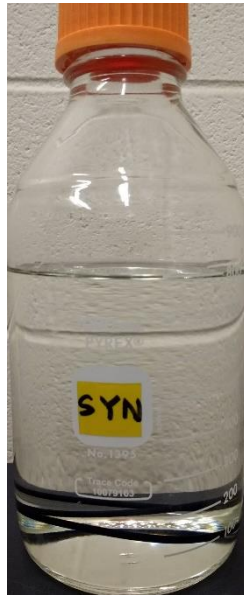


Figure 2-3 EC-100 before testing



Figure 2-4 EC-100 after 6 weeks

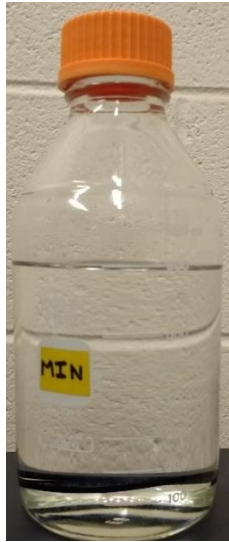


Figure 2-5 mineral oil before testing



Figure 2-6 mineral oil after 6 weeks

Chapter 3

DYNAMIC MECHANICAL ANALYSIS

3.1. Overview

Stiffening of samples taken from various components of IT equipment and immersed in mineral oil, as part of our ongoing research into oil-immersion cooling [3,5], has resulted from increase in Young's modulus over time. Hence, it is one of the best indicators of changes in mechanical properties of polymeric materials immersed in oil. This is substantiated by results reported by A Leal-Junior et al [27]. Furthermore, the maximum allowable effective bending stress in a cable is contingent upon the elastic modulus of the cable as a whole [23].

Based on the literature review, the scope for testing optical fiber relevant to thermal aging under oil-immersion includes, but is not limited to:

- Aging of fiber core due to propagation of surface flaws
- Aging of coating materials
- Fiber/cable strength and fatigue testing

Essentially, the objective here is to develop a test method for studying evolution of mechanical properties (weight, E, CTE, Tg, etc.) over time if there are changes induced in the jacket material or fiber coating due to chemical interactions with the mineral and synthetic oil. This is achieved by the dynamic characterization of the cumulative viscoelastic properties of the cable specimens.

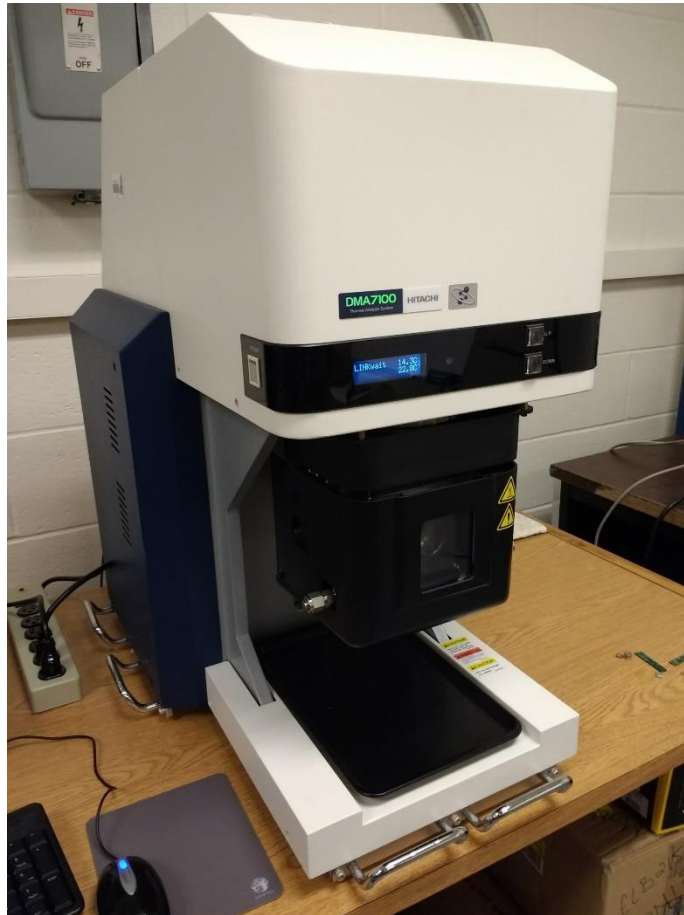


Figure 3-1 The DMA used

3.2. Apparatus

For the purpose of analyzing the change in thermomechanical properties of the cable samples, a Hitachi DMA7100 Dynamic Mechanical Analyzer was used. Viscoelastic properties like E^* (complex modulus), E' (storage modulus), E'' (loss modulus) and $\tan\delta$ (loss tangent) were recorded and analyzed in the inbuilt TA7000 software in the computer that interfaces with the DMA. The frequency and temperature-dependent complex moduli, and glass transition can be obtained from the DMA. The use of dynamic mechanical instrumentation for characterizing the viscoelastic properties of thermoplastic and thermosetting polymeric materials has been extensive in studying reliability of IT equipment

[13,14,15,16,17]. The elastic modulus data generated may be used to identify the thermomechanical behavior change over time in immersed, aging environment. Determination of the modulus as a function of furnace temperature was made according to ASTM D 5418.

3.3. Specimen Preparation

After each of the four cycles ended, 15 cm sections were cut out of the longer 50 cm sections of cables from each jar. Subsequently, three specimens were carefully cut from said 15 cm sections, and immense care was exercised while cutting to make sure that no yellow yarn strands (presumably the strength member or strain relief member in the cable), were pulled out, so that both the fibers were intact, and any possible inaccuracy was avoided.



Figure 3-2 Air-exposed sample



Figure 3-3 Oil-immersed sample

Particulars of the tested specimens and DMA conditions are as follows:

Sample shape: Circular

Sample length: 50 mm

Geometry factor: $7.007\text{E-}005$ m

Average outer diameter: 2.9 mm

Mode: dual cantilever bending

Separation between probe and jaw: 20 mm

Force amplitude: 100 mN

Strain amplitude: $20\mu\text{m}$ (0.1% strain)

Scanned at two frequencies: 1 and 5 Hz

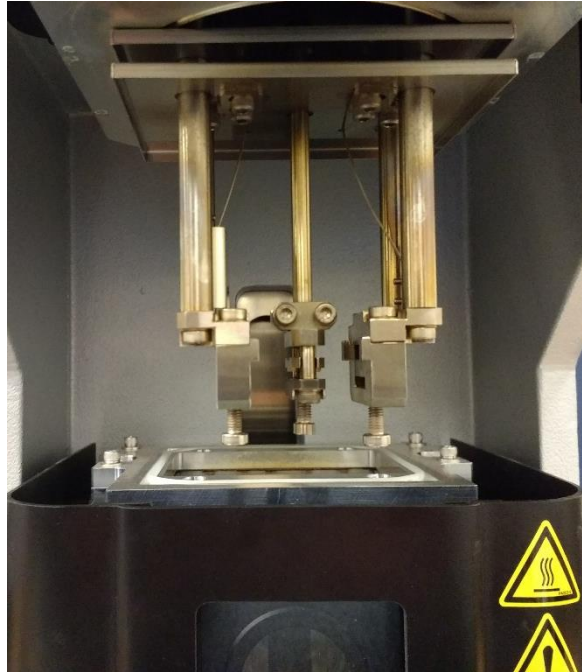


Figure 3-4 Sample-holding jaw and probe

Start temperature: 20°C

End temperature: 80°C

Ramp rate: 10°C/min

Data sampling rate: every 3.0 s

The choice of 1Hz was based on the reports of viscoelastic properties of data cables tested in literature. A frequency scan required at least an additional frequency of 5 Hz would allow studying molecular weight and distribution trends of the molecular weight.

The elastic-dominant behavior is better observed at higher frequencies, and a frequency scan at multiple frequencies can be used to perform for time-temperature superposition (TTS) to estimate cable life.

The upper limit of the DMA furnace temperature of 80°C affords the opportunity to observe viscoelastic behavior near glass transition temperature (T_g) of PVC. Additionally, since maximum continuous-use temperature of PVC is 70°C, it is important that the PVC not start getting affected in any manner that overtake the effects caused by thermal aging in the oil. Hence, a short term isothermal hold of no more than 80°C should not result in the same. Furthermore, the need to prevent the DMA furnace temperature from rising to a point where the value of the Young's modulus became lower than the analyzer's given resolution, led to the decision of not surpassing 80°C and getting dangerously close to the T_g of PVC.

3.4 Observations

There was no appreciable change in length of sample post-removal from DMA furnace. Hence, one can infer that there was no problem with jaw gripping the sample ends. There were no anomalies in the Lissajous curves: in line with expected stress-strain behavior.

Oil was observed on the surface of immersed samples and DMA bending attachment jaw after removal from furnace. It is not plasticizer leaching out since air-exposed specimen surface was completely dry after removal (refer to figures 3-5 and 3-6)



Figure 3-5 Oil-immersed sample after removal from DMA



Figure 3-6 Air-exposed sample after removal from DMA

3.5 Results

3.5.1. Elastic Modulus (E^*)

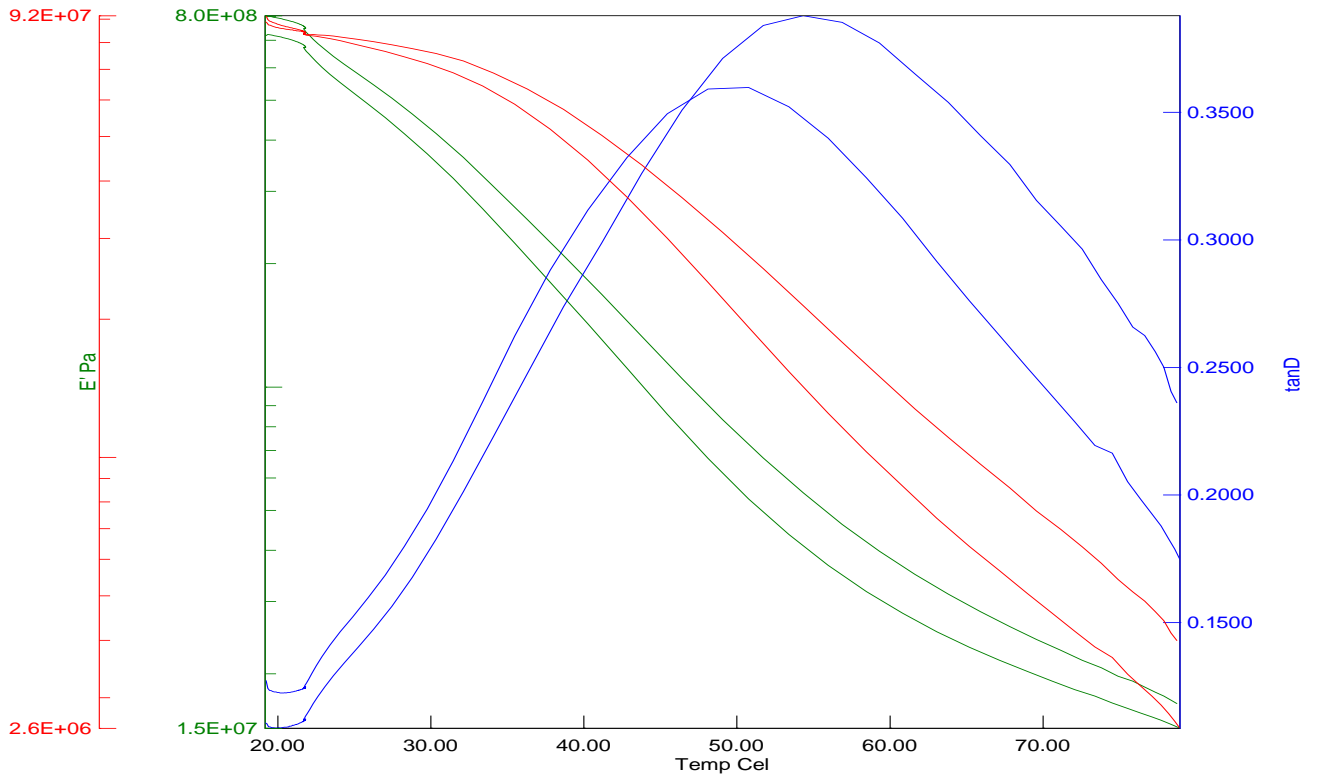


Figure 3-7 Response of mineral oil-immersed sample scanned at 1 & 5Hz after 2nd cycle

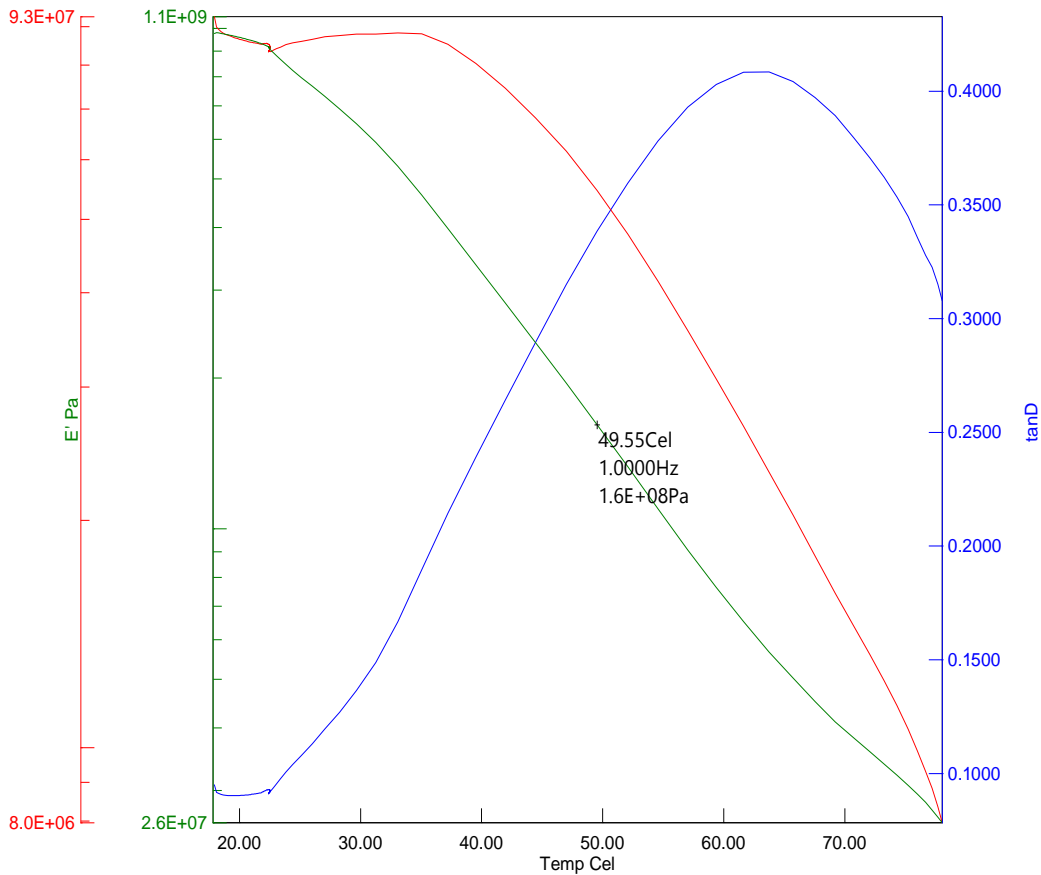


Figure 3-8 Response of EC-100-immersed sample @ 1Hz frequency after 4th cycle

The exponential behavior of the elastic complex modulus (E^*) is evident in figures 3-10 and 3-11. It is in agreement with Young's modulus-temperature correlation reported by A Leal-Junior et al [27] (figure 3-9). They report that dynamic elastic modulus exhibits high variation with temperature for temperatures below 80°C. In general, trends of storage modulus (E'), loss modulus (E''), and loss tangent ($\tan\delta$) strongly agree with observations made by Junior et al.

However, complex modulus (E^*) values of distinct samples almost invariably plateaus between 60 and 80°C, which is also where loss tangent($\tan\delta$) peaks.

Agreement between E^* of samples from the same jar and after equal aging time is stronger at higher temperatures ca. 40°C than at near room temperature, which is why values are reported at both room temperature and 40°C.

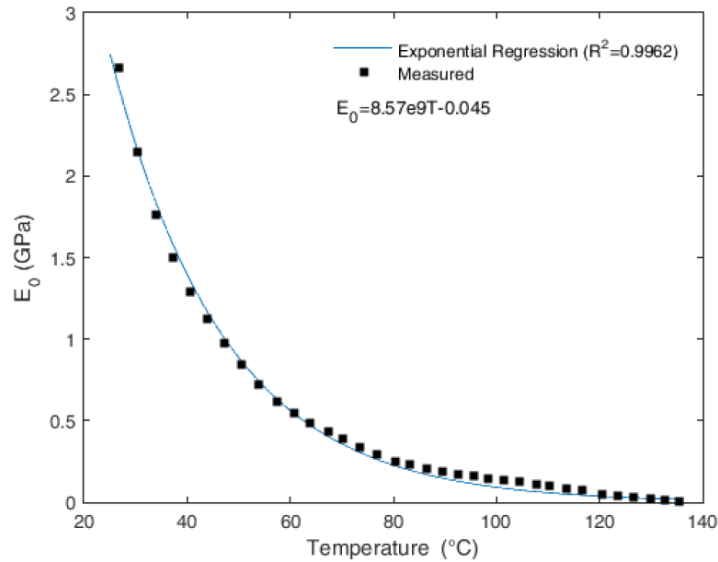
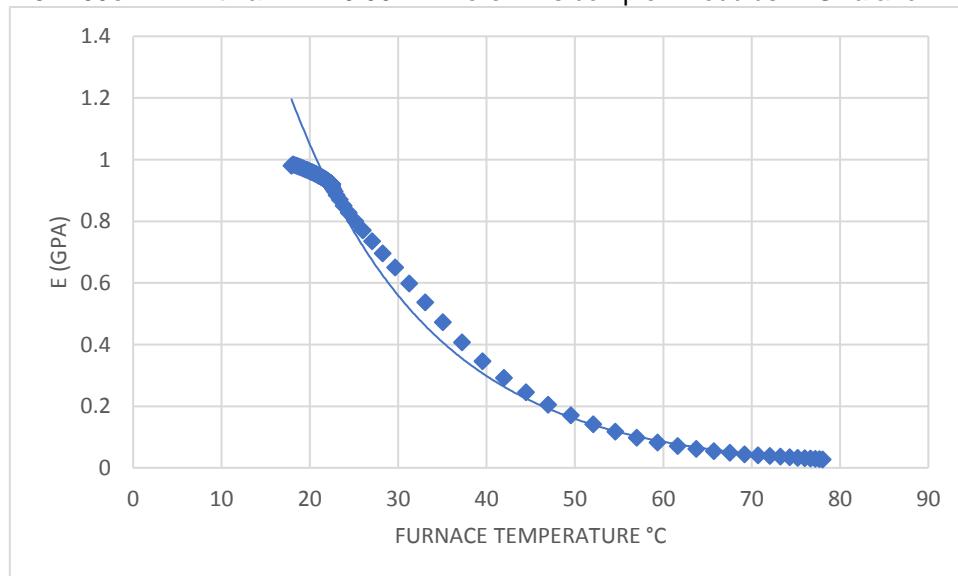


Figure 3-9 E-T correlation for fiberoptic temperature sensor

Figure 3-10 shows the general behavior of the complex modulus of mineral oil-immersed sample after the 3rd cycle, which may be approximated by an exponential function of the form $E^* = 5E+09e^{-0.071T}$ with an $R^2 = 0.9972$ where E^* is complex modulus in GPa and T is



DMA furnace temperature in °C. A similar trend is observed in EC-100-immersed samples after the 4th cycle (figure 3-11)

Figure 3-10 E vs T behavior of mineral oil immersed sample after 3rd cycle

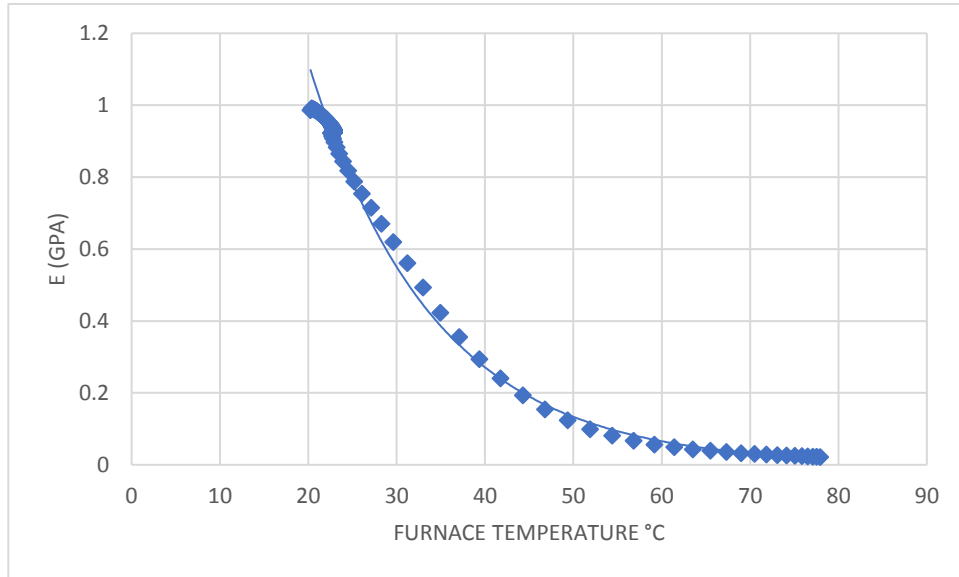


Figure 3-11 E vs T behavior of EC-100 immersed sample after 4th cycle

The “baseline” in table 3-1, refers to the elastic modulus values measured of samples taken from the pristine, unaged cables, otherwise referred to as “as-received” samples. A plot of the values of each specimen is given in figure 3-12. These values are reported at 40°C furnace temperature of the DMA. Similarly, table 3-2 and figure 3-13 report the samples’ viscoelastic response when the furnace is at room temperature (22°C).

Table 3-1 Specimen elastic modulus vs time at 40°C DMA furnace temperature

E (Mpa)				
Cycle	Air-exposed	Mineral oil	EC-100	Baseline
1	22.9	84.5	144	28.57
2	30.7	149.2	253	28.57
3	38.9	294	311	28.57
4	35.9	316.9	321.8	28.57

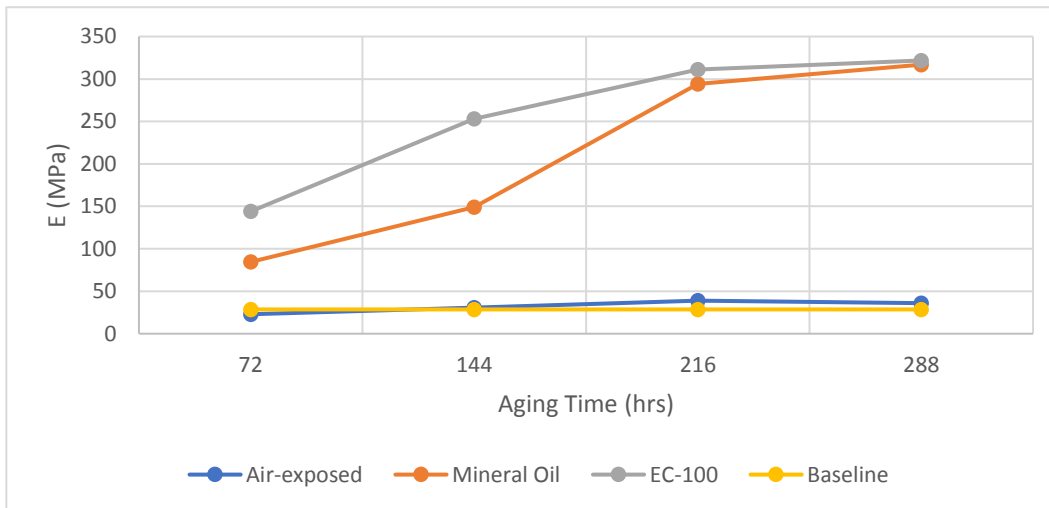


Figure 3-12 Evolution of complex/elastic modulus over aging time at DMA furnace temperature of 40°C

Table 3-2 Specimen elastic modulus vs time at 22°C DMA furnace temperature

E (Mpa)				
Cycle	Air-exposed	Mineral oil	EC-100	Baseline
1	120 ^a	484	676.6	101.35
2	100	653.8	860	101.35
3	102.5	950	945.5	101.35
4	108.3	901.5	930.6	101.35

a The value of E* was inflated due to an error in measured OD of sample (2.85 instead of 2.9 mm)

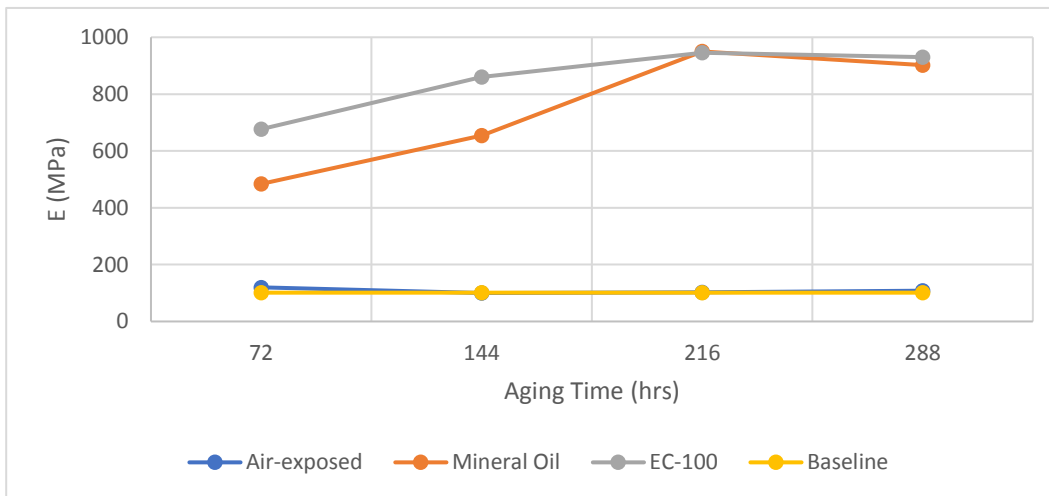


Figure 3-13 Evolution of complex/elastic modulus over aging time at DMA furnace temperature of 22°C

3.5.2 Loss Tangent

The effect of immersion on loss tangent (ratio of storage modulus(E') to loss modulus(E'')) for all samples is tabulated in table 3-3. Upward shift in $\tan\delta$ peaks with increase in aging time is clearly visible for immersed samples, in figure 3-14.

Table 3-3 Loss tangent peaks

Cycle	Air-exposed	Mineral oil	EC-100	Baseline
1	0.33830526	0.35529798	0.361604	0.319697
2	0.30887017	0.35970908	0.382362	0.319697
3	0.28423888	0.39612275	0.398727	0.319697
4	0.29276326	0.39275625	0.408451	0.319697

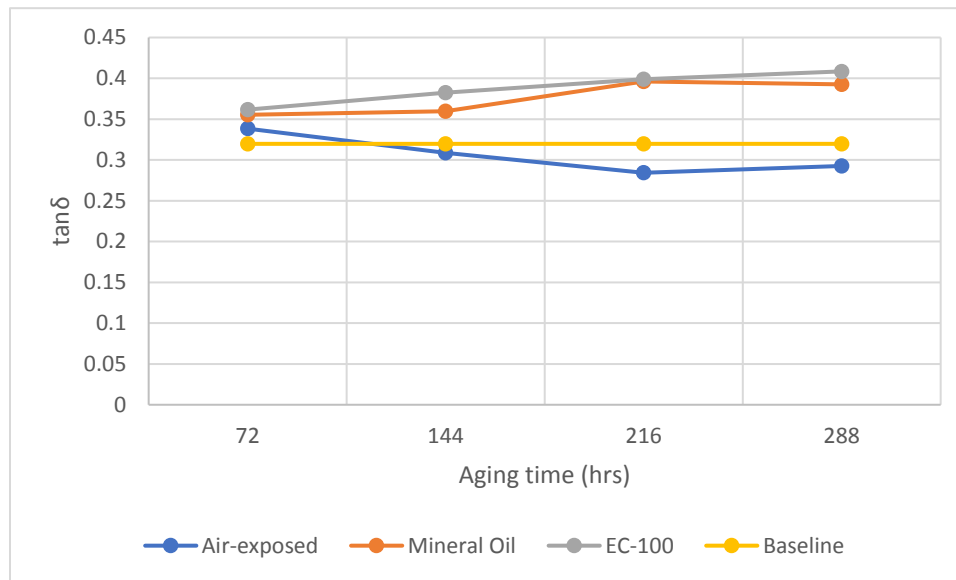


Figure 3-14 $\tan\delta$ peak shifts with aging time

3.7 Theoretical Treatment of Mechanical Effects of Aging

The focus was on evaluating the mechanical properties of jacket and coating material. The cable jacket made of is OFNR-rated polyvinyl chloride.

The degradation mechanism of the thermoplastic PVC jacket due to aging by immersion in high-temperature oil can be formulated from the DMA test results of each specimen. These changes in the viscoelastic properties indicate changes in its macromolecular polymer chain structure.

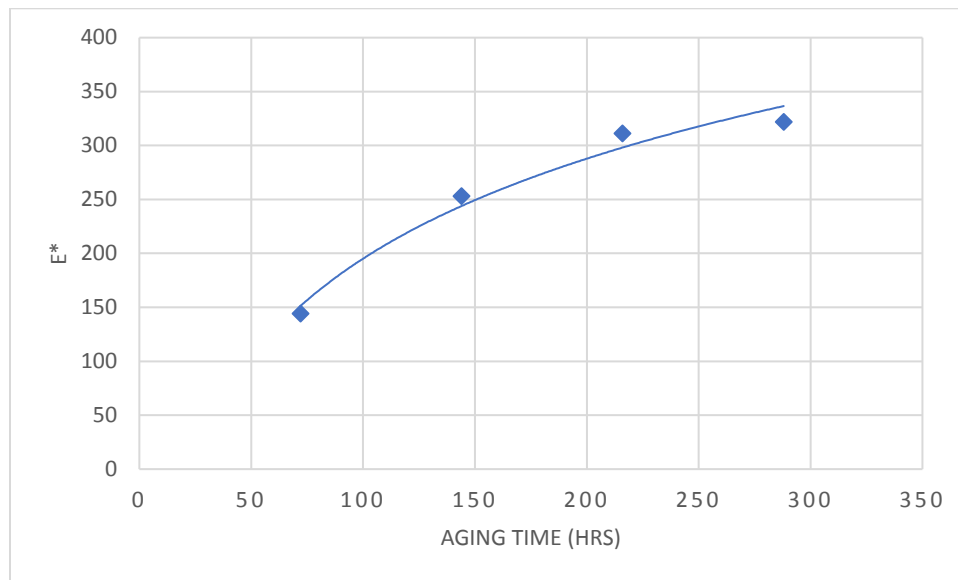


Figure 3-15 Elastic Modulus vs time for EC-100 immersed samples at 40°C furnace temperature

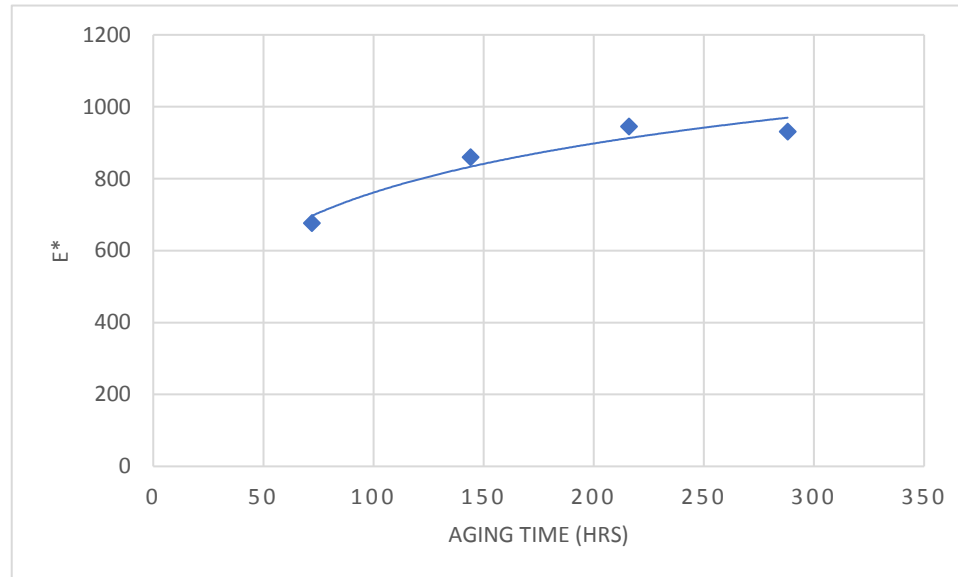


Figure 3-16 Elastic Modulus vs time for EC-100 immersed samples at 22°C furnace temperature

From the logarithmic trends fitted to the data in figures 3-15 and 3-16, it can be hypothesized that the effect of aging is self-limiting and slows down after the first few cycles.

3.7.1 Mechanism of Degradation

PVC jacket hardness is increasing due to plasticizers leaching out and/or ingress through diffusion of oil. Coating toughness rose in magnitude and may contribute to increase in the fiber mechanical strength.

Stiffness and Young's modulus of cable increased with aging time, as hypothesized, and this was in agreement with recent and extant literature.

- $\tan\delta$ peaks upward trend indicates that immersion is causing T_g to elevate and since T_g is strongly dependent on the content of plasticizer* and general polymer chemical state [28], it is reasonable to conclude that some plasticizer leached out into the oil.

Reduction in variation over aging time may be due to two competing phenomena:

- Increased initial diffusion of oil molecules through PVC jacket, and loss of plasticizers due to elevated aging temperature increasing diffusion coefficient, and aggregation of the PVC molecules increasing microvoids. Loss of plasticizer causing PVC molecules to aggregate and allow for more voids for the oil-ingress. High temperatures damage acrylate coatings, which might deteriorate its adhesion to the fiber, causing delamination and exposing the bare fiber to undergo cracking/fractures.
- Increased thermal degradation of fiber coating entails stiffening, reduced ductility, and increased net strength causing diminution in diffusion of oil molecules, as evident from $\tan\delta$ peak shifts

Chapter 4

SURFACE MORPHOLOGY

4.1 Scanning Electron Microscope

The Hitachi S-3000N Scanning Electron Microscope was used.



Figure 4-1 SEM setup

4.2 Cross-section of as-received cable samples



Figure 4-2 View of overall cross section

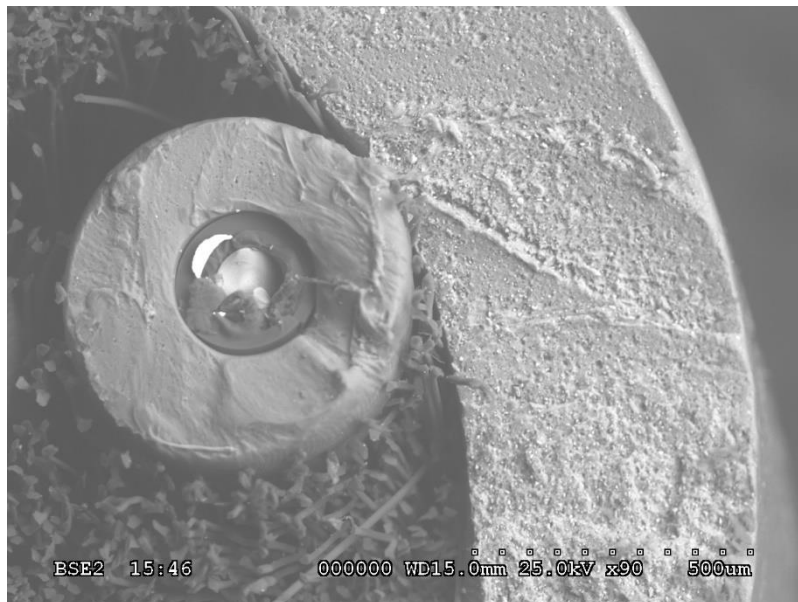


Figure 4-3 Magnified view of core and PVC jacket

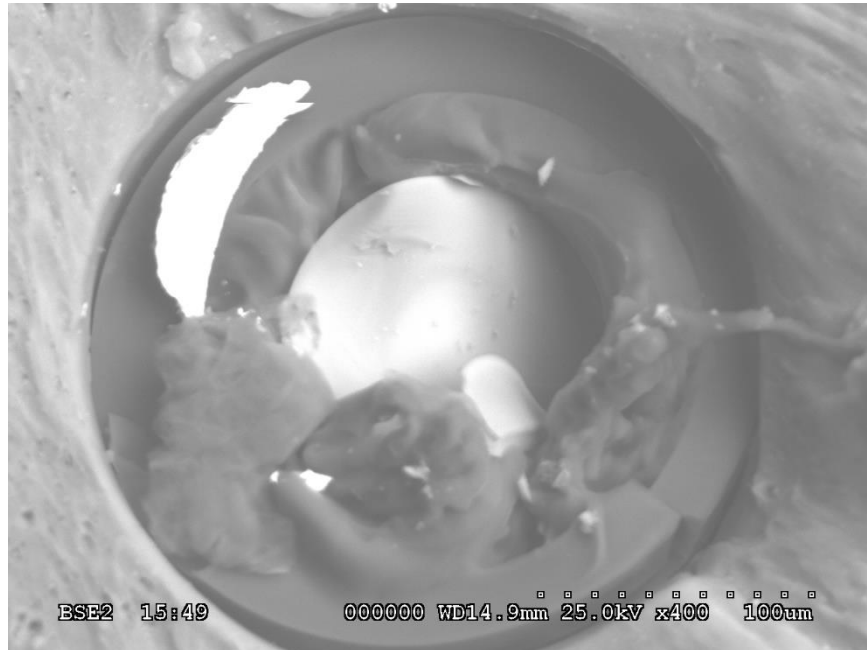


Figure 4-4 One of the two silica cores

It is evident from the micrograph of the cross section of the fiber cores, in figure 4-4, that the core has suffered structural damage. It is important to note that since these images were taken from sections of as-received cable, they were unaffected by aging or immersion, and hence the damage to the core is purely a result of using a tool that is not ideally used for cutting fiberoptic cables. This image closely resembles the SEM image of an optical fiber that was cut with a razor, a tool that is not advisable for cutting fiber cables [26].

The following information is revealed by the SEM images:

- Each core is 50 μm in diameter
- Core-coating thickness is 200 μm
- Cladding thickness is 50 μm

- Jacket thickness is 500 μm
- Strain relief or strength member is presumably aramide yarn

Comparison with oil-immersed sample cross section is required to determine if oil is getting absorbed, causing swelling of cross section. The need for better specimen preparation to resolve substrate adhesion issues is felt as we failed to get the samples to vertically stand on the substrate, thus precluding any further study of the cross section of the immersed samples, restricting the study to that of just surface morphology. This may be because of the failure of the oil-immersed samples to adhere to the adhesive tape used on SEM substrate, as this problem did not occur with the dry, as-received cable samples.

4.3 Air-Exposed Sample after 2nd cycle

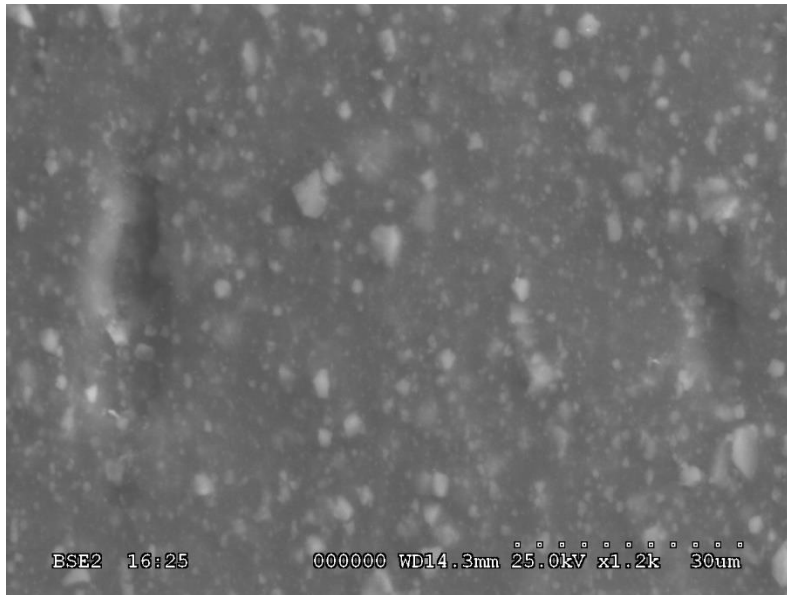


Figure 4-5 1.2K times magnified view of air-exposed sample

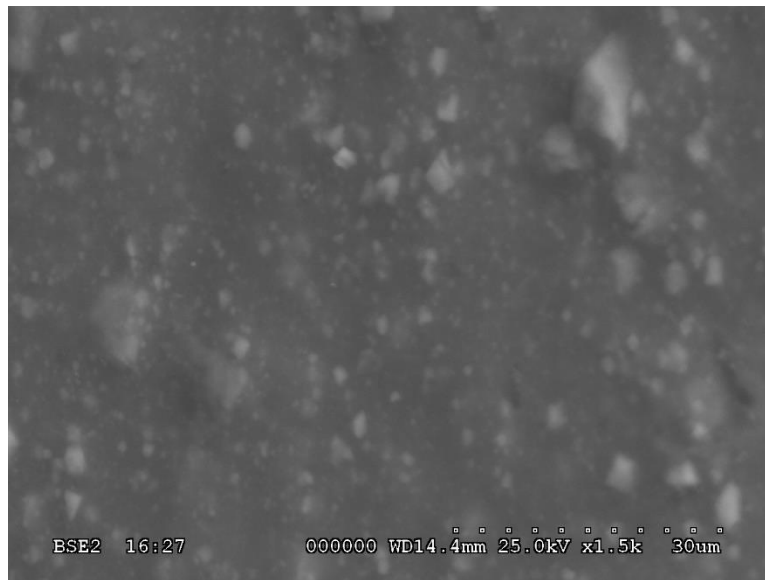


Figure 4-6 1.5K times magnified view of air-exposed sample

Small inorganic filler molecules, plasticizer and microvoids are apparent in both figures. When we compare micrographs of the mineral-oil immersed sample surface morphology with that of the air-exposed, increased microvoids and aggregation of PVC molecules is readily visible. This entails certain positive and negative outcomes, both of which are discussed in chapter 5.

4.4 Mineral Oil-Immersed Sample after 3rd cycle

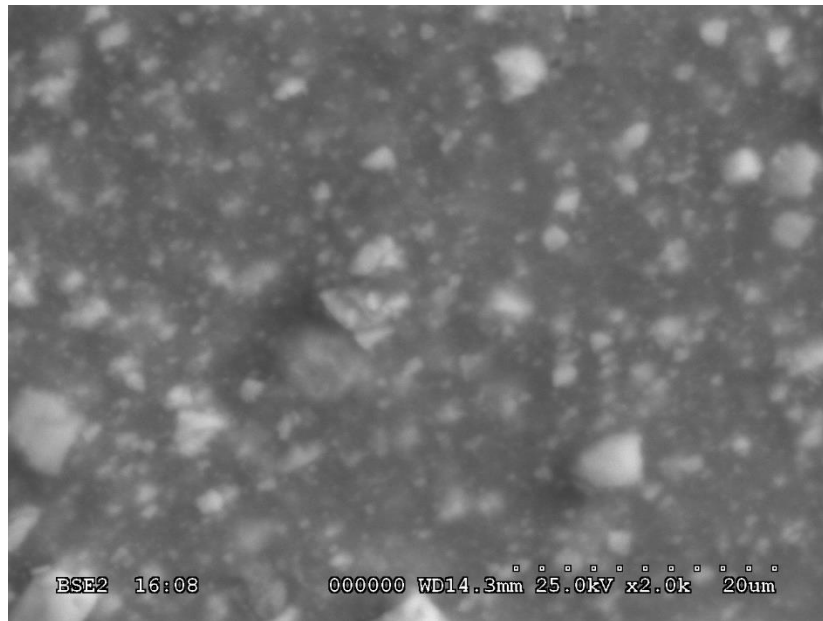


Figure 4-7 2K times magnified view of oil-immersed sample

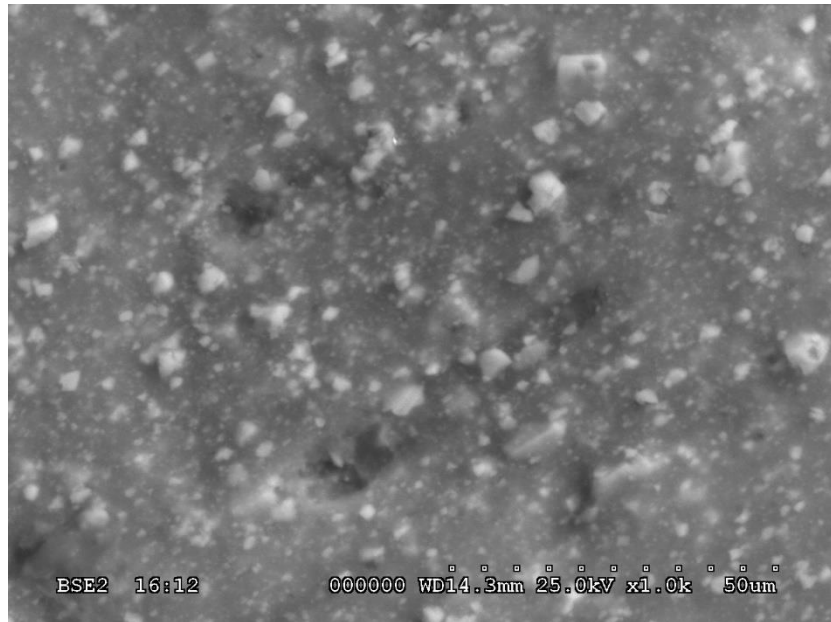


Figure 4-8 1K times magnified view of oil-immersed sample

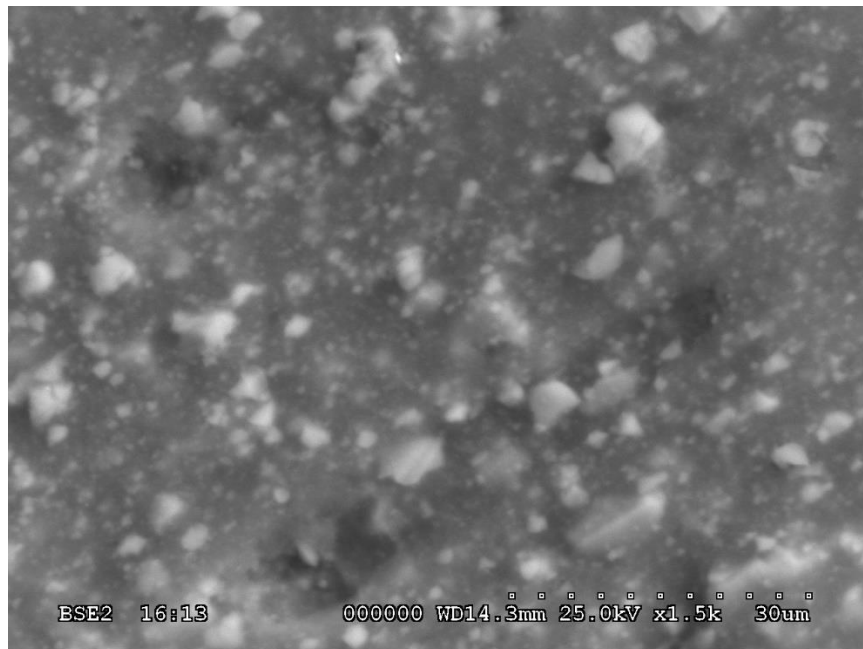


Figure 4-9 1.5K times magnified view of oil-immersed sample

CONCLUSION AND FUTURE WORK

The following conclusions can be made from the analysis:

- Superior fracture toughness, flexibility, and smaller bend radius would be ideal characteristics in silica-core optical cables if oil-immersion is to be used as viable alternative, and while strength degradation is a concern, the results seem to demonstrate that being a self-limiting process, since the coating becoming tougher seems to be temporarily offsetting the damage caused by diffusion of oil through the jacket.
- Clumping together or aggregation of PVC molecules might be an outcome of plasticizer leaching out.
- Coating toughening is a relatively positive outcome as it minimizes transmission losses due to microbending. However, this needs corroboration by optical loss testing.
- Similar tests need to be repeated at higher aging temperatures, so as to determine a single-process dependent phenomenological exponential Arrhenius model, based on chemical reaction kinetics of the oil-PVC interaction. Since this testing was performed at a single aging temperature of 45°C, there are not nearly enough data points to develop a first order Arrhenius-type model to the temperature-dependence of cable performance.

Some issues that need to be addressed in the future are:

- Need for better specimen preparation to resolve substrate adhesion issues

- Need to modify the grips in tensile stress proof testing to prevent any slippage during future testing.

The scope for future work is vast:

- Tensile strength testing: to determine if fiber strength follows a trend similar to that of elastic modulus
- FTIR spectroscopy to assess changes in composition along with spectral imaging to visualize material distribution, and corroborate proposed mechanism.
- Sensitive and accurate glass transition temperature determination, as this would define the limits of utilizing oil-immersion cooling.
- Repeating DMA tests at multiple frequency scans, to study molecular weight distribution and the change thereof. Trends at 1 and 5 Hz were not sufficient to make significant conclusions.
- Performing time-temperature superposition (TTS) on DMA
- Bending tests, to calculate aging-time and temperature dependence of bending radius. Mechanical failure is dependent on bending radius, as outlined by a bending stress model in Osamu et al [23] about the maximum allowable effective bending stress. The Young's modulus of the optical fiber, the radius of the glass region of the optical fiber, bending radius are variables influencing bending stress.
- Multi-physics simulation results to validate theoretical model
- Spectrometer-assisted signal transmission testing to study changes in attenuation characteristics caused by thermal aging in oil. It would also serve to bolster the hypothesis of coating toughness increase lowering signal attenuation.

References

1. S. Sakr, A. Liu, D. Batista, and M. Alomari, "A Survey of Large Scale Data Management Approaches in Cloud Environments," *IEEE Commun. Surveys & Tutorials*, vol. 13, no. 3, pp. 311–336, Jul. 2011.
2. J. M. Shah, R. Eiland, A. Siddarth and D. Agonafer, "Effects of mineral oil immersion cooling on IT equipment reliability and reliability enhancements to data center operations," 2016 15th IEEE Intersociety Conference on Thermal and Thermomechanical Phenomena in Electronic Systems (ITherm), Las Vegas, NV, 2016, pp. 316-325.
doi: 10.1109/ITHERM.2016.7517566
3. Singh P, Klein L, Agonafer D, Shah JM, Pujara KD. Effect of Relative Humidity, Temperature and Gaseous and Particulate Contaminations on Information Technology Equipment Reliability. ASME. International Electronic Packaging Technical Conference and Exhibition, Volume 1: Thermal Management ():V001T09A015. doi:10.1115/IPACK2015-48176
4. J. Shah et al., "Critical non-thermal consideration for oil cooled data-center" in IMAPS ATW 2015, Los Gatos, Ca, 2015.
5. Jimil M. Shah, Dereje Agonafer, "Issue on Operational Efficiency for Oil Immersion Cooled Data Centers" in Session Co- Chair and Presenter for ASME Panel On "Thermal Management Challenges in Energy Conversion & Conservation" ASME IMECE 2015, Houston, Texas.
6. Jimil M. Shah, "Reliability challenges in airside economization and oil immersion cooling", The University of Texas at Arlington, May 2016.
7. Shah JM, Awe O, Agarwal P, et al. Qualitative Study of Cumulative Corrosion Damage of IT Equipment in a Data Center Utilizing Air-Side Economizer. ASME.

- ASME International Mechanical Engineering Congress and Exposition, Volume 10: Micro- and Nano-Systems Engineering and Packaging():V010T13A052. doi:10.1115/IMECE2016-66199.
8. Shah JM, Awe O, Gebrehiwot B, et al. Qualitative Study of Cumulative Corrosion Damage of Information Technology Equipment in a Data Center Utilizing Air-Side Economizer Operating in Recommended and Expanded ASHRAE Envelope. ASME. J. Electron. Packag. 2017;139(2):020903-020903-11. doi:10.1115/1.4036363.
 9. <http://www.steoil.com/msds-tech-data>
 10. D. Godfrey and W. R. Herguth, "Physical and Chemical Properties of Industrial Mineral Oils Affecting Lubrication, Parts 1-5," Society of Tribologists and Lubrication Engineers, Park Ridge, IL, 1996.
 11. <http://multimedia.3m.com/mws/media/910896O/datacenter-dynamics-paris-obi-cooling.pdf>
 12. http://www.panduit.com/ccurl/150/459/FiberOpAppGuide2011_GU_ENET-TD003A-EN-E_ENG,0.pdf
 13. Unique Rahangdale, B Conjeevaram, Aniruddha Doiphode, Pavan Rajmane, Abel Misrak, Dereje Agonafer "Solder ball reliability assessment of WLCSP—Power cycling versus thermal cycling" IEEE International Thermal and Thermomechanical Phenomena in Electronic Systems (ITherm), 2017.
 14. Unique Rahangdale, R Srinivas, S Krishnamurthy, Pavan Rajmane, Abel Misrak, Dereje Agonafer "Effect of PCB thickness on solder joint reliability of Quad Flat no-lead assembly under Power Cycling and Thermal Cycling" SEMI-THERM, 33rd Symposium 2017.

15. Unique Rahangdale, Aniruddha Doiphode, Pavan Rajmane, Abel Misrak, Dereje Agonafer "Structural integrity optimization of 3D TSV package by analyzing crack behavior at TSV and BEOL" Information and Communication Technology, Electronics and Microelectronics (MIPRO), 2017 40th International Convention.
16. Unique Rahangdale, Pavan Rajmane, Abel Misrak, Dereje Agonafer "Reliability Analysis of Ultra-Low-K Large-Die Package and Wire Bond Chip Package on Varying Structural Parameter Under Thermal Loading" ASME INTERPACK 2017.
17. Unique Rahangdale, Pavan Rajmane, Abel Misrak, Dereje Agonafer "A Computational Approach to Study the Impact of PCB Thickness on QFN Assembly Under Drop Testing With Package Power Supply" ASME INTERPACK 2017.
18. Glaesemann, G. S., S. T. Gulati, and J. D. Helfinstine. "Effect of strain and surface composition on Young's modulus of optical fibers." Optical Fiber Communication Conference. Optical Society of America, 1988.
19. Glaesemann, G. S. "The mechanical behavior of large flaws in optical fiber and their role in reliability predictions." Proc. Inter. Wire Cable Symp. Vol. 41. 1992.
20. Dwivedi, Anurag, G. Scott Glaesemann, and C. K. Eoll. "Optical Fiber Strength, Fatigue and Handleability After Aging in a Cable." IWCS Proc. 1994.
21. Volotinen, Tarja T., and Osman S. Gebizlioglu. "Mechanical behavior of coated fused silica optical fibers aged at elevated temperature in air and filling compound." Optical Network Engineering and Integrity. Vol. 2611. International Society for Optics and Photonics, 1996.
22. W Griffioen, "Mechanical Lifetime of Optical Fibers ", Proc. 42nd IWCS, pp. 471 - 475 (1993).
23. Aso, Osamu, et al. "Inference of the Optical Fiber Lifetime for Mechanical Reliability." Furukawa Review 42 (2012): 1-6.

24. https://www.corning.com/media/worldwide/coc/documents/Fiber/PI1468_07-14_English.pdf
25. Mauron, Pascal, Ph M. Nellen, and Urs Sennhauser. "High-Temperature Ageing of Modern Polymer-Coated Optical Fibres." MRS Online Proceedings Library Archive 531 (1998).
26. <http://cas2.umkc.edu/physics/sps/news/news0910.html>
27. Leal-Junior, Arnaldo, et al. "A Polymer Optical Fiber Temperature Sensor Based on Material Features." Sensors 18.1 (2018): 301.
28. Crawford, Dawn M., Robert G. Bass, and Thomas W. Haas. "Strain effects on thermal transitions and mechanical properties of thermoplastic polyurethane elastomers." Thermochimica Acta 323.1-2 (1998): 53-63.

Biographical Information

Hrishabh Singh was born in Muzaffarpur, India in 1992. He received his Bachelor of Technology in Mechanical Engineering from Symbiosis International University, India in June 2014, and a Postgraduate Diploma in Renewable Energy at TERI University in July 2015. He completed his Master of Science in Mechanical Engineering from the University of Texas at Arlington in May 2018.

He worked as a Junior Engineer in the Renewables Engineering Department at Aashraya Technologies Pvt. Ltd., Bangalore from December 2014 - January 2016, where his primary responsibilities included conducting technical feasibility and cost-benefit analyses for thermal systems for a host of R&D applications.

He joined the EMNSPC team at UTA in Spring 2017, and was engaged in investigating the reliability and feasibility of cooling optical interconnect systems by immersion in dielectric coolants (mineral and synthetic oil). He was concurrently developing a computational tool to compare Direct, Indirect evaporative cooling and traditional air-cooling in high-density data centers.

Hrishabh is keen to work in the renewable energy industry and is passionate about distributed energy sources and optimizing energy-intensive operations.